

UNIVERSITY OF CINCINNATI

Date: 21st May 2009

I, Amit Kulkarni,

hereby submit this original work as part of the requirements for the degree of:
Master of Science

in Pharmaceutical Sciences

It is entitled:

Surface Modification of Carboxyl-functionalized Polymeric

Nanoparticles for Attachment of Targeting Peptides

Student Signature: Amit Kulkarni

This work and its defense approved by:

Committee Chair: Gerald B. Kasting, Ph.D.

Arthur R. Buckley, Ph.D.

Randall R. Wickett, Ph.D.

Approval of the electronic document:

I have reviewed the Thesis/Dissertation in its final electronic format and certify that it is an accurate copy of the document reviewed and approved by the committee.

Committee Chair signature: Gerald B. Kasting, Ph.D.

Surface Modification of Carboxyl-functionalized Polymeric Nanoparticles for Attachment of Targeting Peptides

A thesis submitted to the
Graduate School
at the University of Cincinnati

in partial fulfillment of the requirements for the degree of

MASTER OF SCIENCE
Graduate Program in Pharmaceutical Sciences

May 2009

by

Amit Kulkarni

M.S. (Biomedical Engineering), State University of New York at Stony Brook, 2003

B.S. (Chemical Engineering), Jawaharlal Nehru Engineering College, India, 1999

Committee Chair: Gerald B. Kasting, Ph.D.

Abstract

Cellular targeting of drug delivery systems represents a promising approach to reduce adverse effects by limiting release of pharmacological agent to desired target site. Controlled surface modification of nanoparticles by specific ligands can facilitate maximum receptor binding and cellular internalization, thereby increasing efficacy of targeting. This research attempts to establish the foundation for ligand-mediated, covalent surface modification of prefabricated carboxyl functionalized polymeric nanoparticles. Control over size and surface charges affecting stability is demonstrated through fabrication of particles in the absence and presence of a stabilizer. Covalent conjugation chemistry for amidation of surface carboxyl groups to amine-bearing ligands is explored and challenges in separating unbound ligands without compromising particle stability are presented. Successful synthesis and purification of a transcytosis-facilitating peptide sequence (-RY**R**GDLGRR-) and its analogues are outlined. Lastly, increased transport of peptide-modified nanoparticles across BeWo cell monolayers, an *in vitro* model of the human placenta is demonstrated. Preliminary competition studies showing this increased transport of peptide-functionalized particles to be a result of receptor mediated interactions are put forth. In summary, we provide sufficient experimental evidence to suggest increased transport properties of modified particles to be dependent on covalent surface conjugation of appropriate ligands. This establishes the foundation to evaluate controlled expression of targeting ligands for optimizing targeting efficiency of delivery systems.

Acknowledgments

First and foremost, I would like to specially acknowledge Dr. Giovanni Pauletti for the opportunity to work with him under his guidance. The present study was entirely conducted with his resources in his laboratory and would not have been possible without his ideas, critique and suggestions.

I would like to express my appreciation to my thesis committee members, colleagues, friends, and family who have supported me and have helped make this thesis possible. Extending my gratitude to my committee members, I am grateful to my supervisory professor, Dr. Gerald Kasting for his consistent support, patience, and advice, Dr. Arthur Buckley for his intellect and valuable suggestions and Dr. Randall Wickett for his time and willingness to serve on my committee and review the document. I would also like to thank Dr. James Knittel and Philip Cherian for their scientific advice and help in the synthesis and purification of the peptides. I am grateful to Dr. Adel Sakr and Dr. Pankaj Desai for their insightful conversations and long-lasting advice about facing and dealing with challenges in life. I am thankful to past and present members of the Pauletti laboratory, especially Santosh Dixit and Saleem Basha from whom I have learnt the most and Shruthi Vaidhyanathan for being a great colleague and friend. The memories and experiences with all my friends: Namrata Barai, Nirmal Bhide, Amy Brown, Jaeyong Cho, Jody Ebanks, Hemali Gunt, Nireesh Hariprasad, Stephanie Harrington, Ganesh Mugundu, Sunila Nair, Dustin Ochoa, Divya Samineni, Radhika Utturkar, Kent Zettel and Grettel Zamora-Estrada will never be forgotten. A special thanks to my closest

friend, Sarah Ibrahim whose constant encouragement, support and contribution cannot be overstated. Most of all, I would like to acknowledge my family for their unconditional love and support. My parents' invaluable guidance provided the bearing in my life and I hope to continue in the example they have set. My father's wisdom and advice will always be remembered, and my mother's love and confidence continues to inspire me. I thank my sister, Aparna Patwardhan for her love, support, and tolerance towards her little brother and my brother-in-law, Ajit Patwardhan for his patience and affection in dealing with me. Finally, but definitely not least, I would like to acknowledge Aditi, my little niece for always believing in her "mamu" and her ability to bring a smile to my face even in the worst of times.

Table of Contents

List of Figures	viii
List of Tables	x
List of Abbreviations	xi
1 Introduction	1
1.1 Significance	1
1.2 Background	1
1.2.1 Peptide Targeting	1
1.2.2 Nanoparticles	3
1.2.3 Surface Modification Chemistry	4
1.2.3.1 Cyanuric Chloride	5
1.2.3.2 EDC	6
1.2.4 Transplacental Transport	7
1.2.4.1 BeWo Cell Monolayer	7
2 Research Objectives	9
2.1 Hypothesis	9
2.2 Specific Aims	9
3 Materials and Methods	10
3.1 Materials	10
3.2 PLGA Nanoparticle Fabrication	10

3.2.1	Particle Characterization	11
3.2.1.1	Size and Zeta Potential	11
3.2.2	Surface Modification	11
3.3	Polystyrene Nanoparticle Characterization	12
3.3.1	Conductometric Titration	12
3.4	Surface Ligand	13
3.4.1	Dansyl Cadaverine	13
3.4.2	Peptide	13
3.4.2.1	Peptide Synthesis	13
3.4.2.2	Peptide Purification	14
3.5	Cell Culture	15
3.6	Transcellular Transport	15
3.7	Statistics	16
4	Results	17
4.1	Poly(D,L-lactic-co-glycolic acid) (PLGA) Nanoparticles	17
4.1.1	Fabrication and Characterization of Nanoparticles	17
4.1.2	Dansyl Cadaverine as Surface Ligand	19
4.1.3	Particle Surface Modification	20
4.1.3.1	Cyanuric Chloride	20
4.1.3.2	EDC	22
4.1.3.2.1	Dialysis	23
4.1.3.2.2	Ultra-filtration	26
4.2	Polystyrene (PS) Nanoparticles	28

4.2.1	Characterization of PS particles	28
4.2.2	Peptide Ligand	29
4.2.2.1	Peptide Synthesis	30
4.2.3	Particle Surface Modification by Fluorescent Peptide	35
4.2.4	Transcellular Transplacental Transport	36
5	Discussion	38
6	Future Directions	47
7	References	48
8	Appendix	53

List of Figures

Reaction Scheme 1: Cyanuric chloride-mediated amidation of carboxylic groups	5
Reaction Scheme 2: EDC-mediated amidation of carboxylic groups	6
Figure 1: Structure of Dansyl Cadaverine	19
Figure 2: Fluorescence intensities of increasing concentrations of DC in solution	20
Figure 3: Effect of cyanuric chloride coupling technology on PLGA particle associated DC	21
Figure 4: Effect of EDC coupling technology on PLGA particle-associated DC	22
Figure 5: Effect of 10% (v/v) methanol dialysis on PLGA particle-associated DC	25
Figure 6: Effect of ultra-filtration on PLGA particle-associated DC	26
Figure 7: Conductometric titration of carboxyl PS particles with NaOH	29
Figure 8: Spectrometric analysis of H-RYRGDLGRR-NH ₂ peptide	31
Figure 9: HPLC chromatograms of H-RYRGDLGRR-NH ₂ peptide	31
Figure 10: HPLC chromatograms of Ac-RYRGDLGRR-NH ₂ peptide	32
Figure 11: Spectrometric analysis of Ac-RYRGDLGRR-NH ₂ peptide	33
Figure 12: LC chromatograms of H-YRGDLGRK(FAM)-NH ₂ peptide	34
Figure 13: Spectrometric analysis of H-YRGDLGRK(FAM)-NH ₂ peptide	34

Figure 14: Transport of fluorescent PS particles with and without surface conjugated RGD peptide across BeWo cell monolayers 36

Figure 15: Transport of fluorescent PS particles with surface conjugated RGD peptide across BeWo cell monolayers in absence and presence of 1mM competitive RGD peptide 37

List of Tables

Table 1: Synthesized peptide sequence analogues	14
Table 2: Characterization of PLGA (no surfactant) particles in water	17
Table 3: Characterization of PVA-containing PLGA particles in water	18
Table 4: Particle properties of DC associated PLGA particles in water	23
Table 5: Effect of methanol concentration on PLGA particle sizes	24
Table 6: Effect of purification technique on PLGA particle sizes	27
Table 7: Characterization of peptide associated PS particles in water	35

List of Abbreviations

AUC	Area Under Curve
DC	Dansyl Cadaverine
EDC	1-ethyl-3-[3-dimethylaminopropyl] carbodiimide
FAM	5(6)-carboxyfluorescein
Fmoc	9-fluorenylmethoxycarbonyl
HPLC	High Performance Liquid Chromatography
NHS	<i>N</i> -hydroxysuccinimide
PLGA	Poly(D,L-lactic-co-glycolic acid)
PVA	Polyvinyl alcohol
PS	Polystyrene
RGD	Arginine-Glycine-Aspartic Acid

1 Introduction

1.1 Significance

Targeted delivery of therapeutic agents to intended tissues and cells can decrease overall required doses and reduce associated side effects. Functionalized biodegradable nanoparticles are a promising approach to accomplish this objective. The targeting ability of a nanoparticle system is represented by its surface properties, by which it may establish specific and/or nonspecific interactions with target cells [1]. Cell-specific interactions of nanoparticles can be achieved by attaching relevant ligands on their surfaces. The efficiency of interaction of these attached surface ligands with their respective receptors is controlled by the natural cellular conformation and valency of the receptors [2]. Hence for successful application, targeted nanoparticles need to be designed carefully so as to correctly express an optimal number of ligands on their surfaces for interaction with receptors.

1.2 Background

1.2.1 Peptide Targeting

Though the concept of targeted drug carriers with high affinity for specific organs, tissues, and cells was introduced in 1906, it has been gaining much attention recently [3]. A serious handicap in the development of targeted systems however has been their rapid removal from the bloodstream to the liver and spleen by cells lining the reticuloendothelial system (RES) [4]. To avoid the RES, a hydrophilic surface and small

particle size under 100 nm are the most often mentioned criteria. Nanoparticle surfaces have been modified with hydrophilic components such as PEG to increase their blood circulation times, resulting in greater concentrations at target site [1, 8]. These carriers are however limited in their ability to deliver a sufficiently high concentration of incorporated drug at targeted site, resulting in low therapeutic efficacy and eliciting undesirable systemic adverse effects [4, 5].

Active targeting of drug delivery systems, based on the increased affinity between a targeting moiety and desired organ can be achieved by attachment of targeting molecules that can recognize and bind to cells onto their surfaces. Combinatorial approaches such as peptide libraries ($\sim 10^{11}$ peptide sequences) on bacteriophages have led to recent successes in the discovery of short peptides that are able to bind to targeted proteins, cells, or tissues specifically [6-10]. Use of short chain peptides as targeting ligands offer multiple advantages in their relatively smaller sizes, ease of manufacture and modification, simple conjugation techniques and cost effectiveness [11].

Peptide ligands targeted to unique membrane proteins, such as receptors, can regulate not only cellular recognition, but also the intracellular trafficking pathway and sub-cellular localization within the cell. Receptor-mediated interactions allow for rapid and increased means of internalization of conjugated carriers in comparison to untargeted complexes [12]. Cell adhesion receptors, such as integrins can be specifically recognized by peptides carrying Arginine–Glycine–Aspartic acid (RGD) motifs, which then internalize by clathrin dependent endocytosis after binding [13]. Dynamic distribution of integrins and conformational changes on binding to RGD motifs can

regulate multipoint attachments through clustering [14]. Polyvalent interactions, involving simultaneous binding of multiple ligands to multiple receptors can be collectively much stronger than predicted by the sum of corresponding monovalent interactions [15]. Thus, peptides displayed on surfaces can exhibit strong receptor binding affinity and desirable targeting efficacy by exploiting multivalent ligand-to-receptor interactions.

1.2.2 Nanoparticles

Nanoparticles offer the opportunity for expression of multiple ligands due to their large surface areas. This can be used to control the number and orientation of the ligand molecules, thereby allowing optimal expression to facilitate maximum ligand-receptor interactions. On account of their small size, they can also penetrate into tissues and small capillaries and offer unique advantages including improvements in target-to-non-target concentration ratios, increased residence at target site, and improved cellular uptake and intracellular stability [16, 17], . Nanoparticles can be made from a variety of organic and inorganic materials including non-degradable and biodegradable polymers, lipids, self-assembling amphiphilic molecules, dendrimers, and metals [18, 19]. For nanoparticles used in drug delivery, biodegradable polymers are advantageous due to versatility for formulation, sustained release properties, sub-cellular size and biocompatibility with tissues and cells [20].

Traditionally, methods to express ligands on particles employ physical adsorption on surfaces of prefabricated particles or covalent conjugation to polymers *prior* to formation of the particles. Physically adsorbed ligands, being mainly dependent on electrostatic interactions, can however come off under physiological conditions thereby limiting the active targeting of delivery systems [21-23]. Covalently linking ligands to polymers first and then manufacturing the particles can expose sensitive ligands to harsh organic conditions, ligands being incorporated inside the particles, and/or possible failure of particle formation due to chemical incompatibility of the ligands and polymers [24]. Therefore, there exists a need for establishing techniques for the covalent surface modification of pre-formed particles to ligands under relatively “mild” conditions.

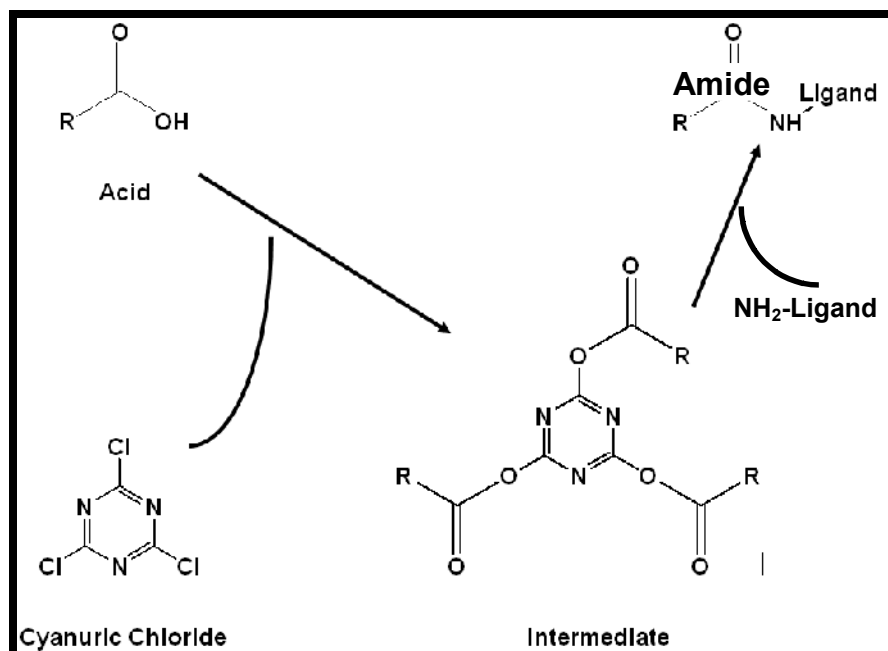
1.2.3 Surface Modification Chemistry

Prior to attachment of ligands, biodegradable polymers made of polyesters such as polylactic acid (PLA), polyglycolic acid (PGA) and poly(lactic-co-glycolic-acid) (PLGA) terminating in carboxylic acid groups need to be activated. Activated carboxyl groups can be readily reacted with amines to form stable amide linkages. Due to their kinetic stability to hydrolysis, amidation reactions offer an attractive alternative for the covalent coupling of ligands to particles under aqueous conditions [25]. Availability and easy access of the N-terminal primary amines of peptides make them the preferred groups for these reactions. Use of the terminal end-groups for conjugation can also allow “free” expression of the peptides for interaction with their respective receptors. Additionally, utilization of the N-terminal amine for immobilization on particle surfaces offers the

opportunity to establish the conjugation chemistry independent of the peptide sequence thereby making it applicable to all peptides or ligands with primary amines.

1.2.3.1 Cyanuric Chloride

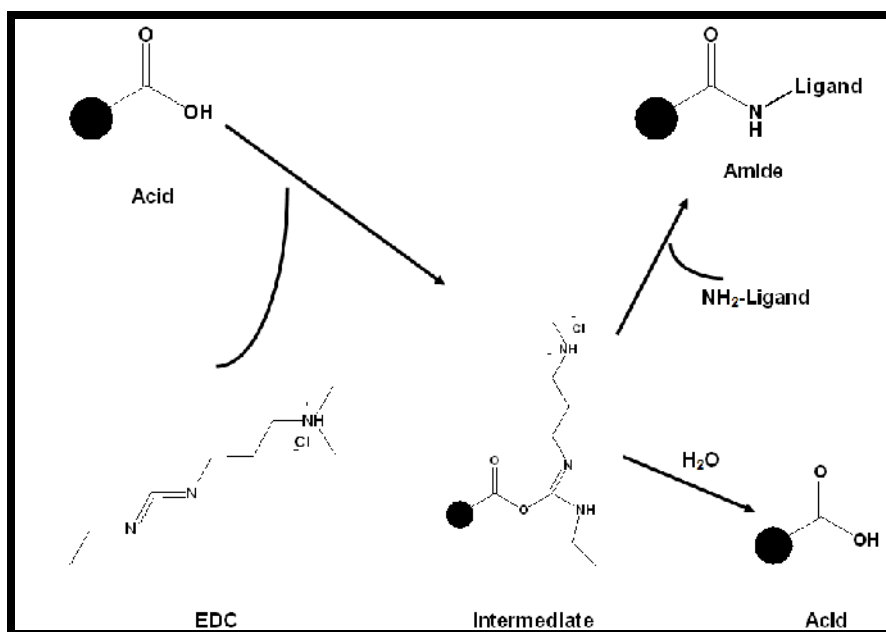
2,4,6-trichloro-1,3,5-triazine (cyanuric chloride), an effective amidation promoter, when treated with a carboxylic acid forms an intermediate which readily reacts with an amine to form the amide and an insoluble hydroxytriazine byproduct readily removed by filtration. The cyanuric chloride-promoted process is advantageous in its minimization of reagent utilization and robust tolerance to presence of water during both the activation and amidation steps [51].



Reaction Scheme 1: Cyanuric chloride-mediated amidation of carboxylic groups

1.2.3.2 EDC

1-Ethyl-3-(3-dimethylaminopropyl)carbodiimide (EDC), a zero-length crosslinking agent reacts with a carboxyl to form an amine-reactive *O*-acylisourea intermediate. This intermediate reacts with nucleophiles, such as primary amines to form amide bonds. Furthermore, in the absence of primary amines, the activated intermediates hydrolyze back to the free carboxyl form [53]. In the presence of *N*-hydroxysulfosuccinimide (NHS), EDC can be used to convert carboxyl groups to amine-reactive NHS esters stable to hydrolysis.



Reaction Scheme 2: EDC-mediated amidation of carboxylic groups

1.2.4 Transplacental Transport

The placenta, a specialized organ constituting the sole structural barrier between the maternal and fetal blood circulation systems regulates processes essential for normal development of the fetus, including the exchange of nutrients and gases and removal of fetal waste products [61]. The syncytiotrophoblast layer comprises the human placental barrier and controls the passage of blood-borne substances from mother to fetus [62]. Passive diffusion of solutes by transcellular and paracellular pathways across this single layer of epithelial cells is the principal mechanism of transfer from maternal blood to fetal blood [63]. As a consequence, for treatment of serious health conditions of the unborn, a critical need exists for the development of clinically effective and safe delivery systems capable of transcytosis across this barrier.

1.2.4.1 BeWo Cells Monolayer

BeWo cells, derived from human choriocarcinoma are monolayer-forming trophoblasts, widely used as a culture system for studying transplacental transport and metabolism *in vitro*. Biochemical similarities of BeWo cells and primary cultures of normal human cytotrophoblasts affirm the use of the cell line for investigations of trans-trophoblast transport of nutrients and drugs [64]. BeWo cells have been shown to be stable, relatively easy to maintain by passage, and to grow to a confluent monolayer in a relatively short period of time, unlike primary human cytotrophoblasts which spontaneously differentiate to a syncytiotrophoblast and do not form a confluent, consistent monolayer [64].

Previously, the peptide sequence (-RY**R**GDLGRR-), was identified by phage display to facilitate transplacental transport of T7 bacteriophages across BeWo cell monolayer, an *in vitro* model of the human placenta [26].

Using the identified peptide sequence and its analogues and other model ligands, we aim to establish conditions for the covalent coupling of ligands to surfaces of prefabricated polymeric particles. We speculate that the expression of the transcytosis-mediating peptide on the particle surfaces will facilitate receptor-mediated interactions of the particles and cells, thereby increasing accumulation and transport of conjugated particles across the *in vitro* barrier.

2 Research Objectives

2.1 Hypothesis

Covalent coupling of integrin-binding RGD peptide (-Y**R**GDLGR-) increases transcellular transport of polymer nanoparticles across the human trophoblast barrier *in vitro*.

2.2 Specific Aims

To accomplish this objective experimentally, we proposed the following aims:

1. To fabricate and characterize stable polymeric nanoparticles
2. To evaluate and synthesize ligands for surface modification of particles
3. To establish surface conjugation chemistry for covalently linking ligands to particles
4. To assess effect of surface modification of particles by peptides on their transport properties across a BeWo cell monolayer.

3 Materials and Methods

3.1 Materials

PLGA RG503H™ was obtained from Boehringer Ingelheim (Ridgefield, CT). Polyvinyl alcohol and Hanks' Balanced Salts (HBSS) were purchased from Sigma Chemicals (St. Louis, MD). Fluorescent and non-fluorescent carboxyl functionalized Polystyrene particles were purchased from Spherotech, Inc (Lake Forest, IL). All amino acids and peptide synthesis reagents were obtained from Aroztech, Inc. (Cincinnati, OH). Cyanuric chloride and Dansyl Cadaverine were purchased from MP Biomedicals (Solon, OH). 1-ethyl-3-[3-dimethylaminopropyl] carbodiimide was obtained from Pierce Biotechnology (Rockford, IL). Ham's F-12 medium, L-glutamine 200 mM (100X), penicillin (10,000 I.U./ml), streptomycin (10,000 µg/ml), and non-essential amino acids 10 mM (100X) in 0.85% saline were purchased from Mediatech (Herndon, VA). Fetal bovine serum was purchased from Valley Biomedical (Winchester, VA). All other chemicals were of high purity or analytical grade and used as received.

3.2 PLGA Nanoparticle Fabrication

200 mg of PLGA RG503H™ polymer (50:50) (MW: 11000 g/mole) was dissolved in 20 ml of acetone. Polymer solution was added drop wise at 1ml/min to 80 ml of deionized water, under controlled stirring (1500 rpm) at room temperature (25°C) followed by additional stirring for 30 minutes. Organic solvent (acetone) was removed at 40°C under reduced pressure (rotary evaporation – 20 mm Hg) for 25 minutes. Suspension was diluted to 1mg/ml with deionized water and characterized for particle size distribution

and zeta potential. Suspension was stored at 4°C until further use. For PVA containing particles, the polymer solution was added to a 0.5% (w/v) PVA solution as the aqueous phase in the second step introduced earlier.

3.2.1 Particle Characterization

3.2.1.1 Size and Zeta Potential

Particle size (dynamic light scattering) and zeta potential measurements were performed on a Malvern Zetasizer[®] Nano series (Worcestershire, UK). Briefly, particle suspension was diluted to 1 mg/ml in deionized water and shaken to ensure uniform distribution. Suspension was measured for particle size distribution in disposable cuvettes and zeta potential in folded capillary cells.

3.2.2 Surface Modification

2 mg/ml (182 µM of carboxyl groups) of PVA-containing PLGA particles were diluted 1:1 in pH 7.4 PBS buffer and incubated with a saturated cyanuric chloride solution (0.44 mg/ml) in water for 24 hours at room temperature in presence of 25-fold molar excess of dansyl cadaverine. For EDC activation experiments, particles were incubated with 2mM EDC and 5mM NHS in PBS for 30 minutes before addition of DC. Particles were then dialyzed against dialysis medium for 24 hours with replacement of dialysate every 8 hours. Particle suspensions were then quantified for associated fluorescence intensities on a BMG Labtech POLARstar[™] OPTIMA series (Durham, NC) (Ex: 330, Em: 520 nm)

and normalized to initial fluorescence added. For ultra-filtration of particles, particles were spun at 5000 x g for 5 minutes using Millipore Amicon[®] Ultra (Billerica, MA) ultra-filtration tubes.

3.3 Polystyrene Nanoparticle Characterization

3.3.1 Conductometric Titration

Standard sodium hydroxide and hydrochloric acid solutions (100 mM) were volumetrically diluted to 1mM and 80 μ M respectively. 50 ml of 80 μ M HCl added to 500 μ l of 0.02% sodium azide was titrated against twenty five, 250 μ l additions of 1 mM NaOH each. Conductivity was monitored after each addition using a pH/Con 510 series oakton meter (Vernon Hills, IL), allowing sufficient time for stabilization of readings. Titration of PS particles was performed similarly by addition of 500 μ l of 50 mg/ml PS suspension (in 0.02% sodium azide) to 50 ml of 80 μ M HCl. Titration end point was determined as the intersection point of the linear slopes of individual titration curve legs. The linear slope of each leg of the titration curve was determined independently as the extrapolation from first data point to last statistically similar data point. Statistical differences between slopes of initial point and consecutive points were determined by student's t-test in individual steps.

3.4 Surface Ligand

3.4.1 Dansyl Cadaverine

Dansyl cadaverine was dissolved in pure methanol at 10 mg/ml for all experiments and used directly at appropriate dilutions.

3.4.2 Peptide

3.4.2.1 Peptide Synthesis

Peptide synthesis was performed using standard Fmoc chemistry on a manual shaker. General synthesis procedure is as described: 1 g of Rink-amide resin (0.75 mmole/g) was swollen for 1 hour in 20 ml of dimethylformamide (DMF), followed by deprotection of Fmoc group with 20% piperidine for 30 minutes, monitored by positive Kaizer test using ninhydrin solution. Resin was washed 3X with 15 ml of alternate DMF and methanol cycles each to remove all traces of piperidine. 2.5 fold molar excess of appropriate amino acid was added along with coupling agent hydroxybenzotriazole (HOBt), base N-methylmorpholine (NMM) and reacted for 60-90 minutes to completion, determined by Kaizer test. Washing and de-protection steps were repeated for addition of other amino acids. Following complete chain synthesis, peptide was washed 3X in dichloromethane (DCM) and methanol and dried overnight before cleavage from resin, using 95% trifluoroacetic acid (TFA) for 2 hours. Crude peptide was precipitated in diethyl ether after evaporation of TFA and film was dissolved in methanol for purification.

Fluorescent peptide was similarly synthesized with a final step coupling of 5(6)-carboxyfluorescein (FAM) to the ϵ -lysine before cleavage from resin.

Nomenclature	Peptide Sequence Analogues	Mol. Weight [g/mole]
Non-fluorescent un-acetylated	H -RYRGDLGRR-NH ₂	1375.50
Non-fluorescent acetylated	Ac -RYRGDLGRR-NH ₂	1417.54
Fluorescent truncated un-acetylated	H -YRGDLGRK(FAM)-NH ₂	1321.40

Table 1: Synthesized peptide sequence analogues

3.4.2.2 Peptide Purification

Spectrometric analysis of peptide was conducted on a Waters 2695 ESI Mass-Spectrometer (Milford, MA) for molecular weight determination, using a 50:50 acetonitrile: 0.1% formic acid mixture for injection. Peptides were analyzed on a Thermo Separations (Waltham, MA) HPLC and a UV 3000, dual wavelength, photodiode array detector. Conditions for analysis were: [C18 column (Varian – 250 mm, 4. Mm I.D.), 25 minute run, solvent A: 0.1% phosphoric acid, solvent B: acetonitrile (gradient: solvent B: 5% to 95% in 20 minutes), 1ml/minute, detection wavelength: 215 nm]. Conditions for preparatory HPLC were: [C18 column, 50 minute run, solvent A: 0.1% TFA in water, solvent B: acetonitrile (gradient: solvent B: 5% to 95% in 45 minutes), 60 ml/minute,

detection wavelength: 215 nm], LC/MS conditions were: [C18 column, 18 minute run, solvent A: 0.1% formic acid, solvent B: acetonitrile (gradient: solvent B: 5% to 95% in 12 minutes), 0.3 ml/minute, detection wavelength: 215 nm]

3.5 Cell Culture

BeWo cells were obtained from American Type Culture Collection (Rockville, MD). The cells were routinely maintained in Ham's F-12 containing 25 mM glucose and supplemented with 1% L-glutamine, 100 I.U./ml penicillin, 100 µg/ml streptomycin, 1% non-essential amino acids and 10% heat-inactivated fetal bovine serum at 37° C in a controlled atmosphere of 5% CO₂ and 90% relative humidity. Experiments were performed using BeWo cells between passages 30-50 . For transport studies, 1 x 10⁵ cells/well were seeded on collagen-coated polycarbonate membranes (Transwell[®], 12 mm in diameter, 0.4 µm pore size) (Costar, Cambridge, MA) and used between 10 and 15 days post-seeding.

3.6 Transcellular Transport

Confluent BeWo cell monolayers were washed 3X with prewarmed HBSS, pH 7.4. Transport experiments were initiated by adding the particle suspension (1mg/ml) to HBSS, pH 7.4 to the apical (AP) compartment (500 µl). HBSS, pH 7.4 (1500 µl) was added to the basolateral (BL) compartment. Samples were periodically removed from the receiver (900 µl) every 15 minutes up to 60 minutes, and fluorescence was

determined by fluorescence intensity measurements using a BMG Labtech POLARstar™ OPTIMA. The sample volume from the receiver was always replaced with fresh, pre-warmed HBSS, pH 7.4.

Apparent permeability coefficients (P_{app}) for particles were calculated according to

$$P_{app} = \frac{\frac{dQ}{dt}}{C \times A}$$

where dQ/dt = linear appearance rate of mass in receiver compartment, C = initial fluorescence concentration in donor compartment, and A = surface area (1.12 cm²)

3.7 Statistics

All experiments were carried out at least in triplicate. Results are reported as mean \pm S.D. Significant statistical differences between groups were evaluated using Student's t-test for two groups or one-way ANOVA for three or more groups (GraphPad Prism 5.02, San Diego, CA).

4 Results

4.1 Poly(D,L-lactic-co-glycolic acid) (PLGA) Nanoparticles

4.1.1 Fabrication and Characterization of Nanoparticles

PLGA RG503H™, a linear polyester polymer, with uncapped carboxyl groups was used to synthesize particles, using the nano-precipitation method. Once synthesized, we characterized the particles for their size distribution, using dynamic light scattering and surface charges, by zeta potential measurements.

	Average Diameter ± Peak Width [nm]	Zeta Potential ± S.D. [mV]
Batch 1	105 ± 41.5	-43.2 ± 4.2
Batch 2	108 ± 40.0	-44.9 ± 5.1
Batch 3	101 ± 43.6	-46.9 ± 4.8

Table 2: Characterization of PLGA (no surfactant) particles in water

Table 2 shows that this fabrication method resulted in PLGA particles with reproducible “nano” size distributions. Additionally, the absence of stabilizers/emulsifiers facilitated preparation of particles exhibiting high negative zeta potential values. This implies presence of free carboxyl groups on particle surfaces, which increases colloidal stability of these particles in suspension. However, changes to suspension conditions required for activation of surface carboxyl groups caused the particles to aggregate and

ultimately precipitate. We concluded from these observations that electrostatic repulsion of the particles under activation conditions was insufficient to prevent aggregation. Therefore, the fabrication protocol was modified to include 0.5% (w/v) polyvinyl alcohol (PVA), a commonly used degradable emulsifier.

	Average Diameter ± Peak Width [nm]	Zeta Potential ± S.D. [mV]
Batch 1	157 ± 49.3	-5.70 ± 4.14
Batch 2	161 ± 50.0	-5.87 ± 4.30
Batch 3	157 ± 46.8	-6.20 ± 3.67

Table 3: Characterization of PVA-containing PLGA particles in water

Particle characterization shows that PVA-containing particles exhibited slightly increased mean diameters with comparable size distributions. Lower zeta potential values suggest shielding of surface carboxyl groups by the incorporated PVA. These PVA-containing particles show no significant change in average diameters and size distributions under activation conditions (data not shown), implying increased stability due to the steric hindrance effect of PVA chains.

Quantification of available surface carboxyl groups for conjugation to ligands is essential to accurately predict coupling reaction efficiency and the valency of ligands present on the surface of each particle. Acid/base titration of particles was employed to quantify the moles of carboxyl groups available for coupling. However, as fabricated PLGA particles

are porous, it is predicted that all exposed carboxyl groups for neutralization with small $-OH$ ions may not accurately reflect carboxyl groups available for surface conjugation with ligand molecules. Theoretical values of carboxyl groups, based on the acid number of the polymer assuming 100 % surface availability were hence used for experiments to determine coupling efficiency.

4.1.2 Dansyl Cadaverine as Surface Ligand

To establish feasible conjugation chemistry between surface exposed carboxyl groups on particles and primary amine groups of ligands, we selected the fluorescent dye, dansyl cadaverine (DC) as a model ligand.

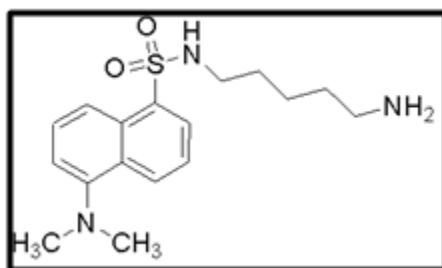


Figure 1: Structure of Dansyl Cadaverine

4.1.3 Particle Surface Modification

4.1.3.1 Cyanuric Chloride

Our initial approach for covalent coupling of carboxyl-functionalized PLGA nanoparticles and fluorescent amine-containing DC ligands focused on 2,4,6-trichloro-1,3,5-triazine (cyanuric chloride) technology. Particle-associated ligands were quantified by fluorescence intensity measurements of DC, after purification by dialysis against water. Figure 2 shows the linearity of the measured fluorescence intensities of DC in solution with increasing concentrations.

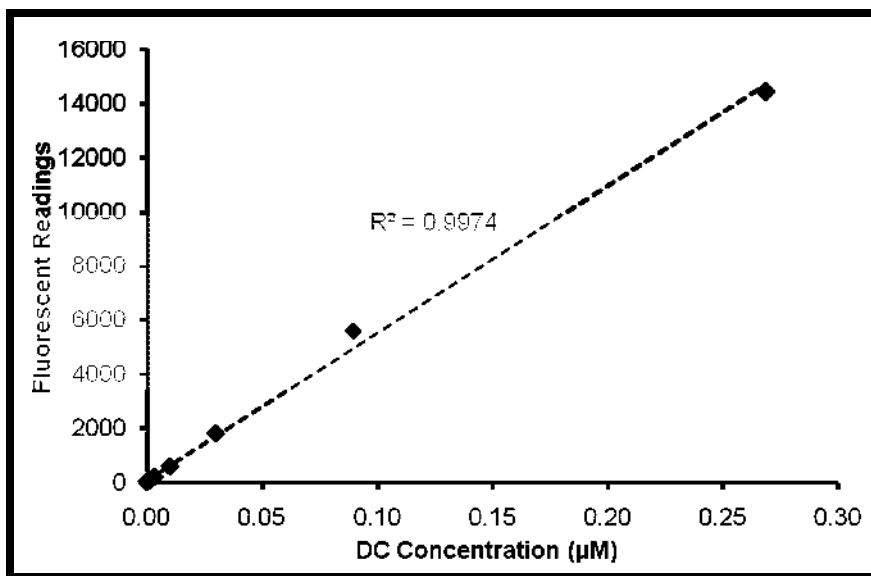


Figure 2: Fluorescence intensities of increasing concentrations of DC in solution. Data are mean \pm S.D. (n=3)

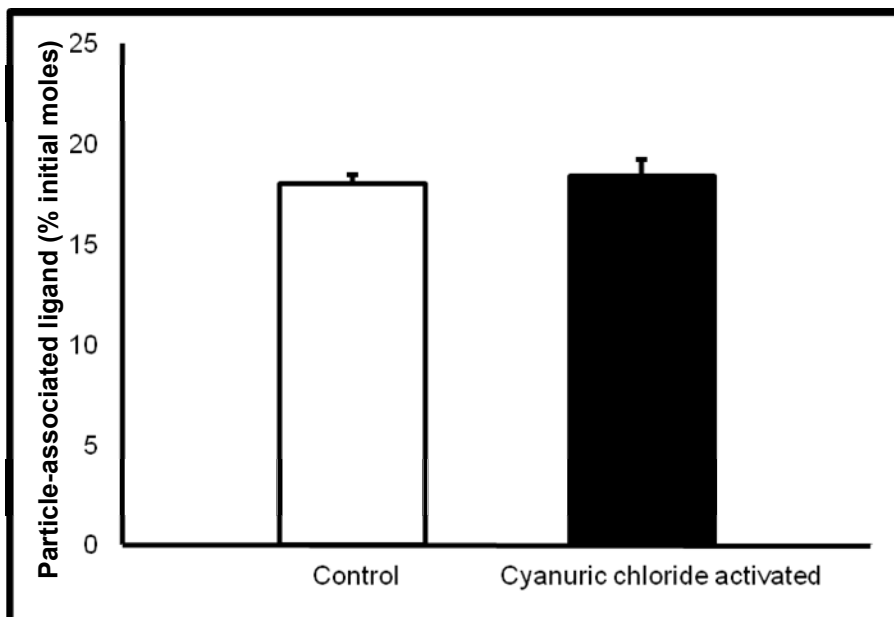


Figure 3: Effect of cyanuric chloride coupling technology on PLGA particle associated DC

DC associated with particles was quantified by measuring the fluorescence intensities of particles after purification and normalizing to initial fluorescence. Data are mean \pm S.D. (n=3)

Figure 3 revealed no significant differences between DC associated with particles, in the absence and presence of cyanuric chloride. Initial DC added to particles was in a 25-fold molar excess to calculated available surface carboxyl groups. We speculate that fluorescence quantification of particle associated DC is not sensitive enough to monitor cyanuric chloride activation of surface carboxyl groups, as explained in the discussion section.

4.1.3.2 EDC

Alternatively, we assessed 1-ethyl-3-[3-dimethylaminopropyl] carbodiimide (EDC) technology for covalent coupling of particle surface carboxyl groups and ligand amine via amidation. Particle-associated ligands were quantified by fluorescence intensity measurements of DC, after purification by dialysis against water. Figure 4 revealed that EDC activated particles showed significantly higher fluorescence. On average, 42% of the 25-fold molar excess DC included in the coupling reaction was recovered on particles after purification. In contrast, ligand associated with PLGA particles without EDC activation was 18%.

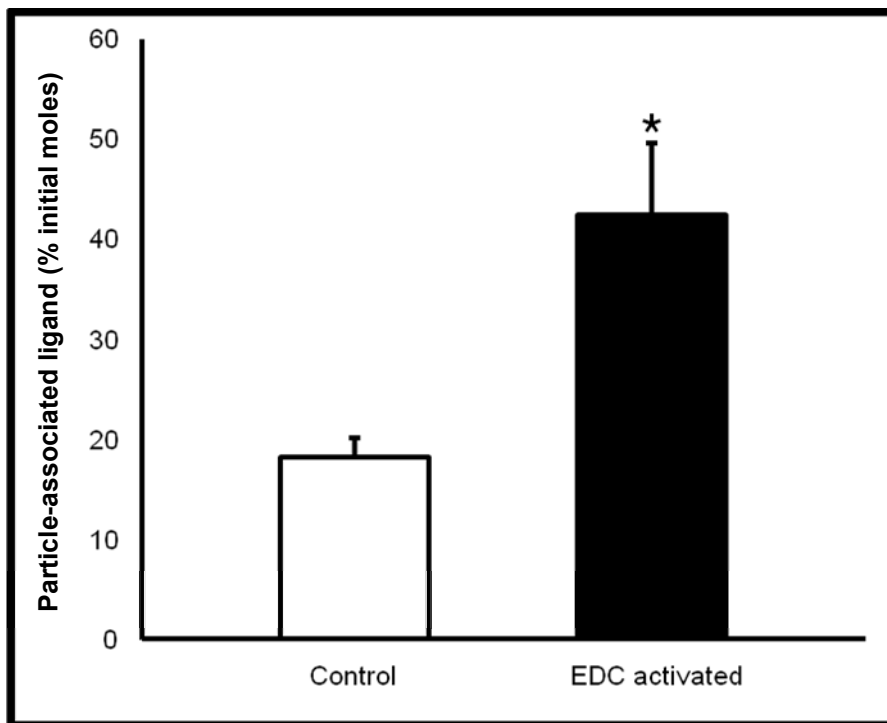


Figure 4: Effect of EDC coupling technology on PLGA particle-associated DC

DC associated with particles was quantified by measuring the fluorescence intensities of particles after purification and normalizing to initial fluorescence. Data are mean \pm S.D. (n=3) (* $p < 0.0001$)

Correlation of the data to molar ratios of DC to carboxyl groups revealed ~ 500% of available carboxyl groups occupied with ligands. These numbers suggest significant non-specific adsorption of DC to PLGA particles in the absence of EDC that persists during applied separation procedures.

Zeta potential measurements of the different particle populations support increased association of DC in the presence of EDC.

	Average Diameter ± S.D. [nm]	Zeta Potential ± S.D. [mV]
Before Activation	158.0 ± 2.3	-5.53 ± 0.94
No Activation (Control)	159.3 ± 10.1	-4.23 ± 0.11
EDC Activated	169.6 ± 17.2	-0.98 ± 0.65*

Table 4: Particle properties of DC associated PLGA particles in water. Data are mean ± S.D. (n=3) (* p < 0.001)

4.1.3.2.1 Dialysis

Efficient removal of non-covalent, surface-associated DC from PLGA particles by dialysis critically depends on the concentration difference between sample and dialysis vehicle that facilitates separation of unbound ligands. Since DC is soluble in pure methanol up to 10 mg/ml and PLGA particle stability is not compromised [27], it was attempted to optimize purification using methanol/water mixtures as dialysis vehicle. We therefore monitored size distribution of PLGA particles following incubation for 24 hours in different concentrations of methanol. Table 5 summarizes the results of these

experiments aimed at identifying optimal dialysis vehicle. Severe particle aggregation and precipitation was observed at methanol concentrations exceeding 50% (v/v). Statistically, though no significant differences were observed in size distributions of particles suspended in $\leq 25\%$ (v/v) methanol, broader distributions and fibrous structures which ultimately precipitated were detected visually in particles suspended in $\geq 15\%$ methanol (v/v). Based on these observations, the concentration of methanol in the dialysis vehicle was limited to 10% (v/v) in subsequent purification attempts.

Methanol Concentration [% v/v]	Average Diameter \pm Peak Width [nm]
0	182 \pm 42.7
10	208 \pm 52.0
15	238 \pm 129
17.5	253 \pm 149
20	250 \pm 117
25	353 \pm 168
35	1460 \pm 469*
50	891 \pm 294*

Table 5: Effect of methanol concentration on PLGA particle sizes (n=4) (* p < 0.0001)

Figure 5 shows that dialysis against 10% (v/v) methanol effectively decreased residual amount of DC associated with PLGA particles in the absence of the activating agent. Fluorescence measurements indicated that ~ 67% of available carboxyl groups remained unmodified. Interestingly, EDC-activated particles maintained a high level of DC comparable to water dialyzed particles (~ 14 fold-excess of available carboxyl groups). These results suggest that, in addition to covalent conjugation of amine containing fluorescent ligands, particles contain a significant fraction of non-covalently bound DC, which cannot be removed by dialysis against 10% (v/v) methanol.

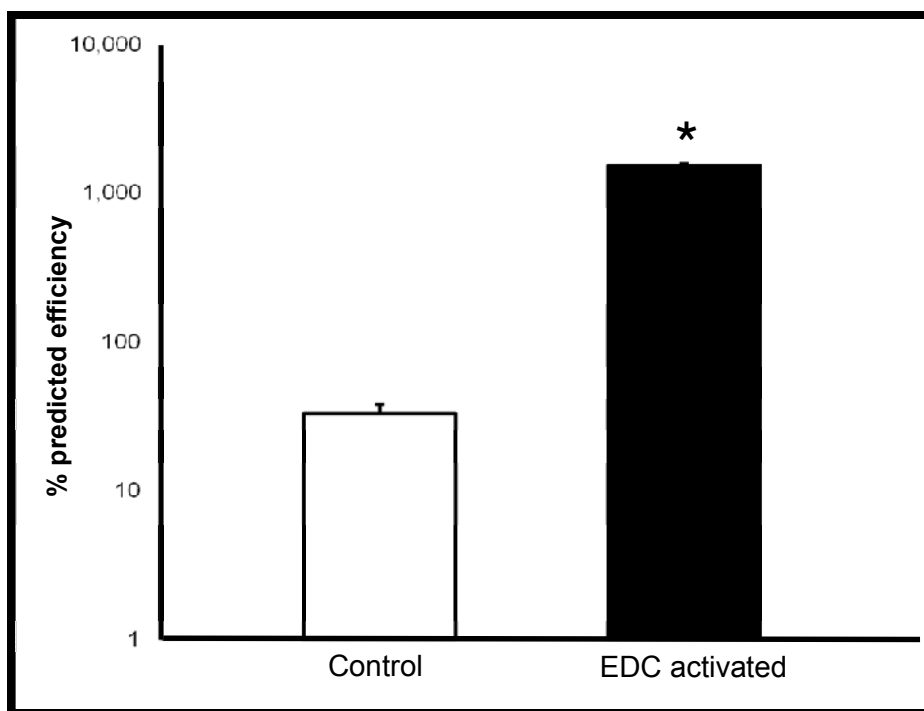


Figure 5: Effect of 10% (v/v) methanol dialysis on PLGA particle-associated DC

DC associated with particles was quantified by measuring the fluorescence intensities after dialysis and normalized to theoretically calculated carboxyl groups, assuming 100% availability. Data are mean \pm S.D. (n=3) (* p < 0.0001)

4.1.3.2.2 Ultra-filtration

To decrease the fraction of non-covalently bound DC on PLGA particles, we explored ultra-filtration (6000-8000 MW cutoff), combined with methanol washes between spin cycles.

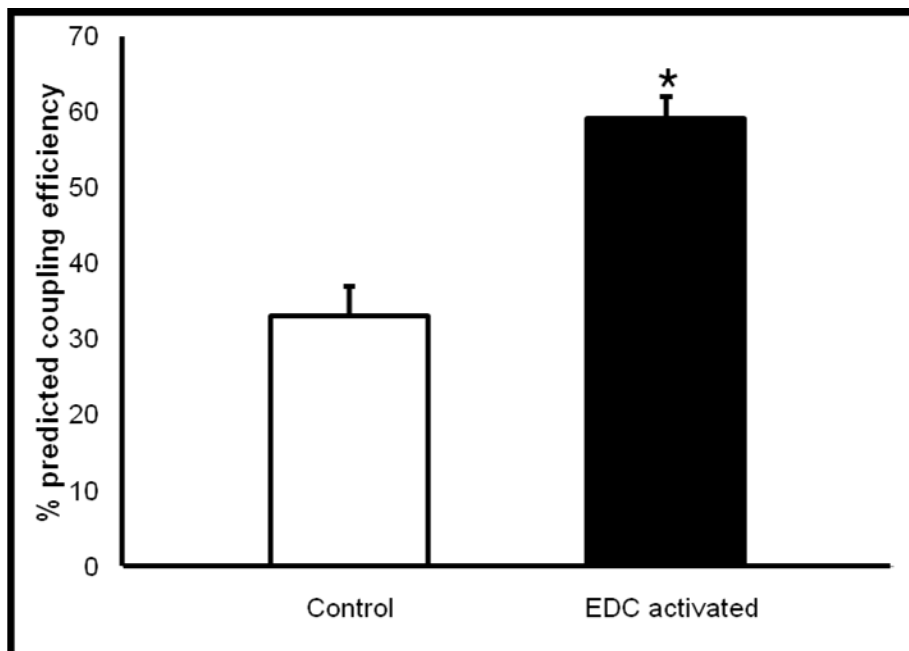


Figure 6: Effect of ultra-filtration on PLGA particle-associated DC

DC associated with particles was quantified by measuring the fluorescence intensities after ultra-filtration and normalized to theoretically calculated carboxyl groups, assuming 100% availability. Data are mean \pm S.D. (n=3) (* p < 0.05)

Results in Figure 6 demonstrate that this method was more successful in separating non-covalently associated DC from particles in contrast to dialysis against water. Predicted coupling efficiency for DC was 33% in the absence and 60% in the presence of EDC as activating agent. Unfortunately, size distribution characterization data, shown in Table 6 indicated significant particle aggregation after ultra-filtration. Attempts to re-

suspend particles to the desired initial nano size range using sonication were unsuccessful.

Average Diameters after ultra-filtration		
[nm]		
Initial	Control	EDC activated
163 ± 5.8	4419 ± 583	5195 ± 486

Table 6: Effect of purification technique on PLGA particle sizes Data are mean ± S.D. (n=3)

Collectively, the results from these studies show that non-covalently associated DC cannot be efficiently removed by dialysis or ultra-filtration using employed conditions, without compromising particle size. We therefore concluded that non-specific hydrophobic interactions of DC with PLGA particles limit its use as a model ligand in our research. Based on these conclusions, choice of ligand was amended to a fluorescent analogue of a hydrophilic peptide.

Additionally, PLGA particle porosity also limited their use in accurately determining coupling efficiency and predicting exact valency of ligands on each particle surface.

4.2 Polystyrene (PS) Nanoparticles

4.2.1 Characterization of PS particles

To circumvent these limitations of fabricated PLGA particles, commercially available non-porous, carboxyl-functionalized polystyrene nanoparticles were obtained. Mean diameters and zeta potential values for the particles were 102 ± 38.8 nm and -61.7 ± 4.7 mV, respectively. Figure 7 shows neutralization endpoint, quantified by the change in conductivity of particle suspension as a function of moles of titrant (NaOH) added. 50 ml of 80 μ M HCl added to particle suspension contributes towards total acid content. Available carboxyl groups at 0.75 μ moles/ 25 mg of PS particles were estimated by the difference in total acid contents of PS particle suspension (3.50 μ moles) and blank sample (2.75 μ moles), respectively.

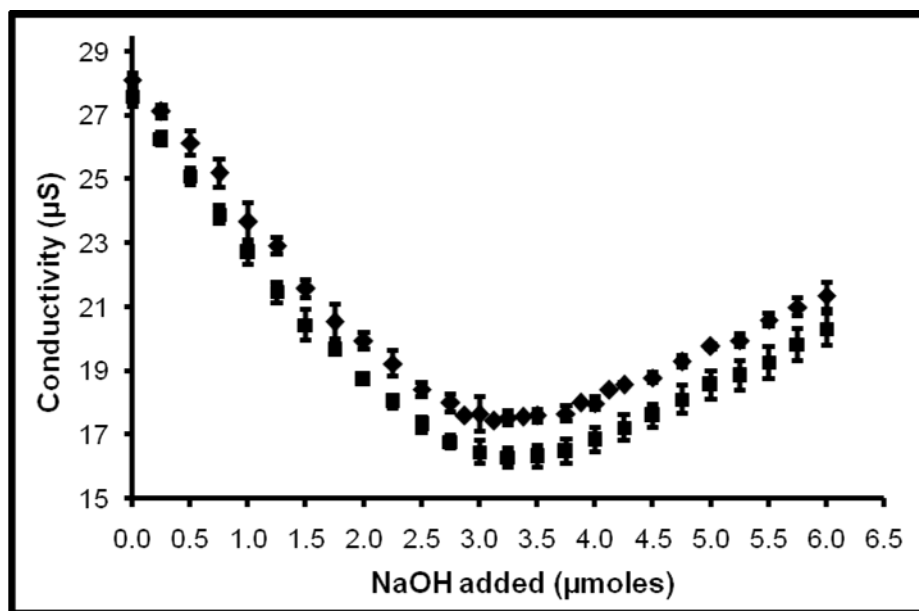


Figure 7: Conductometric titration of carboxyl PS particles with NaOH

Effect of increasing NaOH (Titrant) moles on the conductivity of polystyrene (PS) particle suspension. The total acid content of a sample can be estimated from the intersection of the linearly extrapolated slopes of the titration curve. (■ = Blank, ◆ = Particles)

4.2.2 Peptide Ligand

To overcome the limitations associated with the low-aqueous soluble DC and to demonstrate surface conjugation chemistry to be independent of the physical properties of ligand, we evaluated particle surface modification by a fluorescent analogue of the identified hydrophilic peptide sequence. Non-fluorescent analogues of the peptide sequence were utilized to assess transplacental transport of peptide-surface-modified fluorescent particles.

4.2.2.1 Peptide Synthesis

Peptide synthesis was performed by standard solid phase chemistry on a Rink-amide resin using 9-fluorenylmethoxycarbonyl (Fmoc) amino acids. Following chain elongation, the crude peptide was cleaved from the resin using 95% TFA and purified by HPLC.

A non-fluorescent peptide analogue was synthesized as described in Materials and Methods with a free N-terminal and amidated C-terminal for initial surface modification of fluorescent particles. Crude peptide was separated and purified to individual fragments by preparatory HPLC and molecular weight of each fragment was identified by spectrometric analysis. Spectrometric data in Figure 8 confirms the presence of correct molecular weight peptide fragment. Figure 9 (Panel A) shows the HPLC chromatogram of crude peptide. The peak eluting at 5.368 minutes in the gradient represents the peptide of interest. Chromatogram of purified peptide in Figure 9 (Panel B) revealed shoulder peaks indicating presence of impurities. AUC quantification however showed peptide to be > 95 % pure, deemed sufficient for our research purposes.

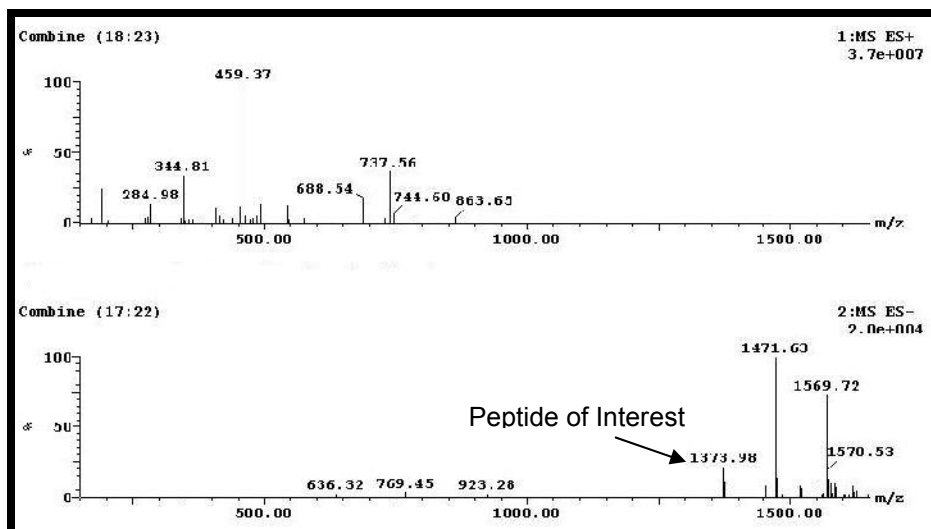


Figure 8: Spectrometric analysis of H-RYRGDLGRR-NH₂ peptide

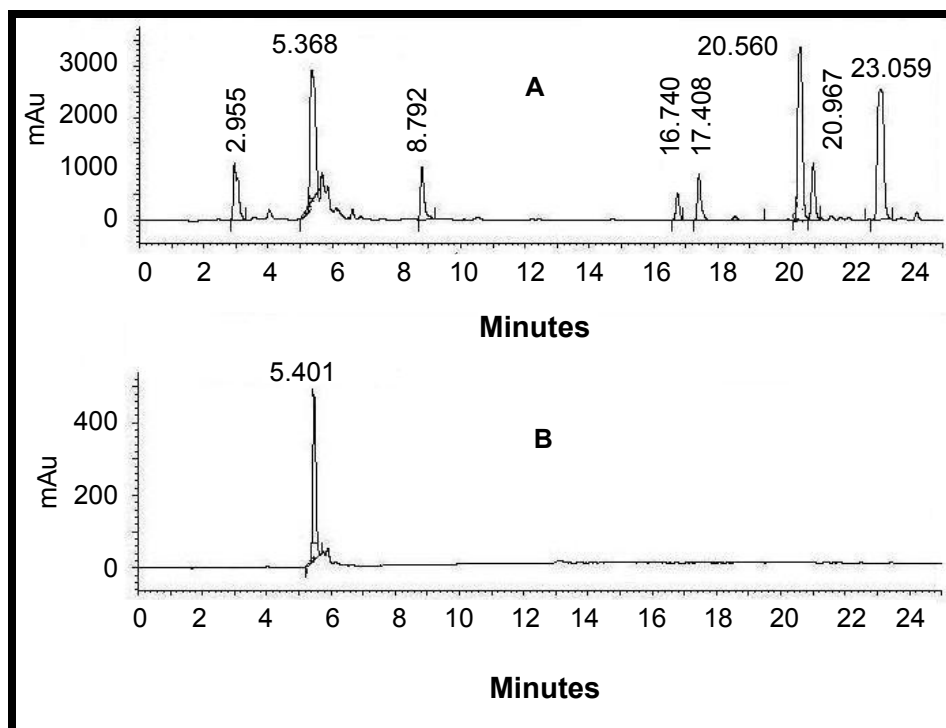


Figure 9: HPLC chromatograms of H-RYRGDLGRR-NH₂ peptide (Panel A: Crude, Panel B: After purification)

A non-fluorescent, N-acetylated and C-amidated peptide analogue was also synthesized, for use as a competitive peptide in the transplacental transport studies of fluorescent particles. Figure 10 displays increased hydrophobicity of the peptide analogue due to N-terminal acetylation, by the shift in peak elution to 6.0 minutes in the gradient. Figure 11 confirms the synthesis of target peptide fragment.

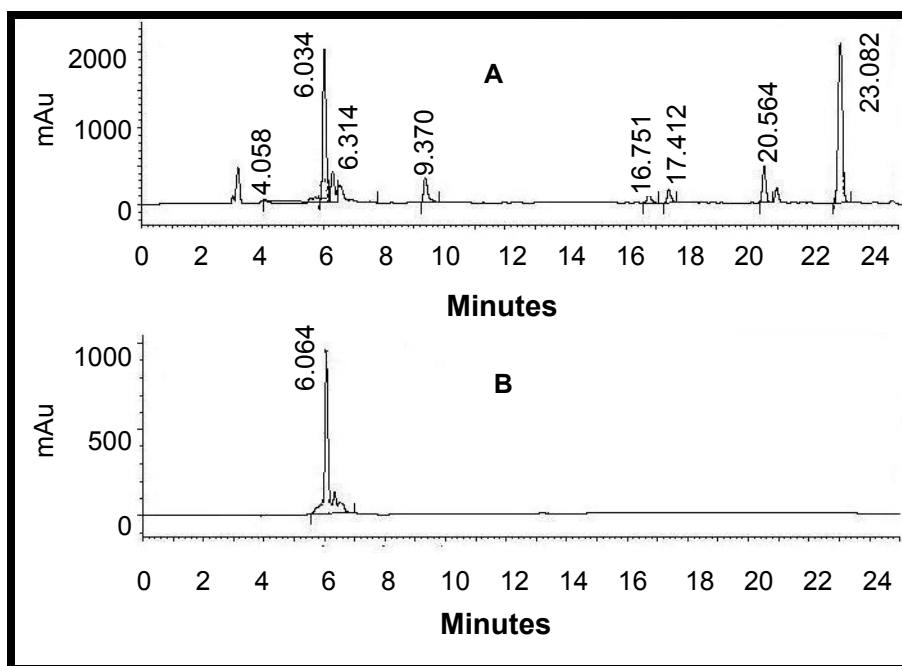


Figure 10: HPLC chromatograms of Ac-RYRGDLGRR-NH₂ peptide (Panel A: Crude, Panel B: After purification)

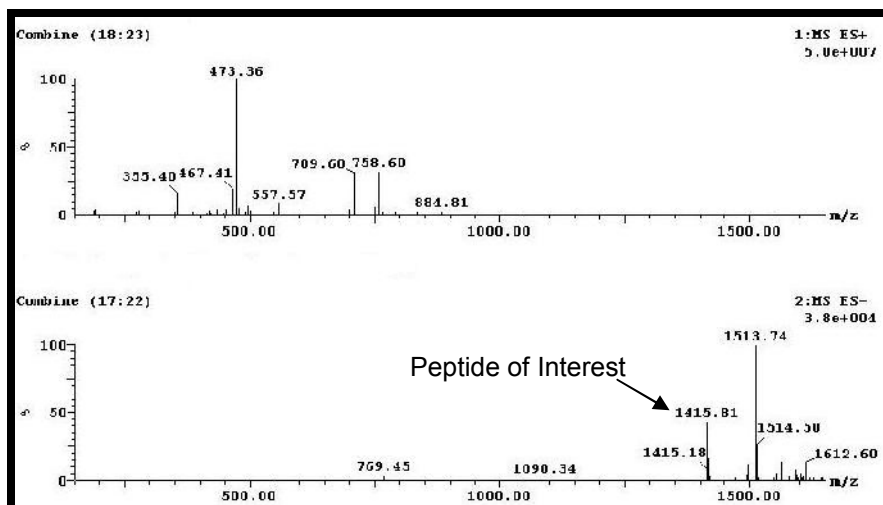


Figure 11: Spectrometric analysis of Ac-RYRGDLGRR-NH₂ peptide

A 5(6)-carboxyfluorescein (FAM) conjugated peptide was synthesized as a fluorescent analogue of the peptide sequence. A truncated version of the peptide sequence (-YRGDLGR-) was used for synthesizing the fluorescent peptide. No statistical difference was observed in the transport facilitating properties between the complete and truncated sequence when tested on phages. FAM was covalently conjugated on the ϵ -amine of the C-terminal lysine as a final step before cleavage, after selective deprotection by 1% TFA. Representative LC chromatograms in Figure 12 and spectrometric analysis in Figure 13 confirm synthesis and purity of relevant fluorescent peptide fragment.

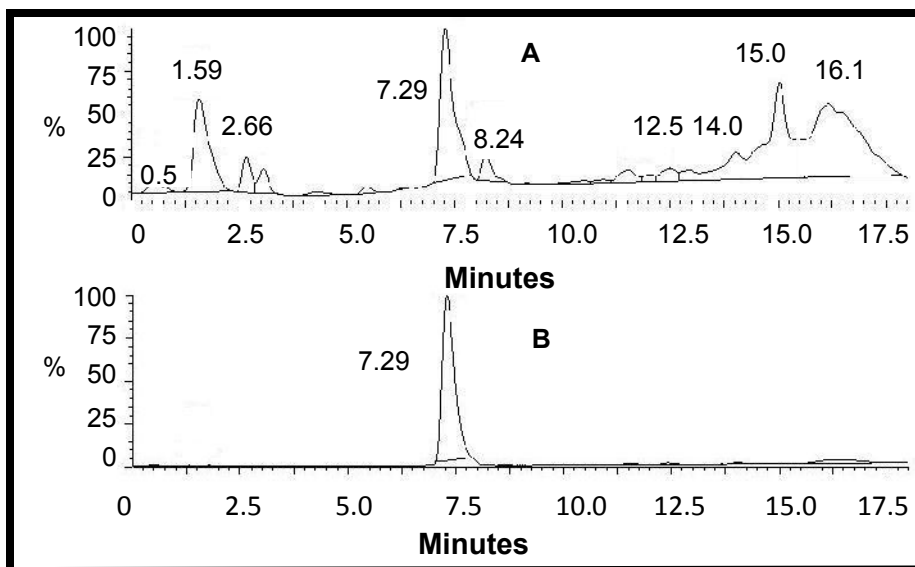


Figure 12: LC chromatograms of H-YRGLGRK(FAM)-NH₂ peptide (Panel A: Crude; Panel B: After purification)

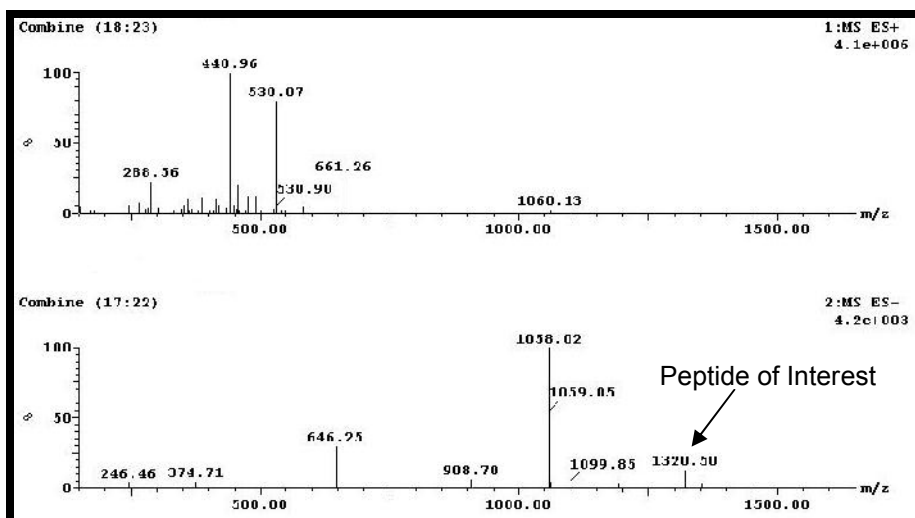


Figure 13: Spectrometric analysis of H-YRGLGRK(FAM)-NH₂ peptide

4.2.3 Particle Surface Modification by Fluorescent Peptide

Surface modification of PS particles by covalent coupling of fluorescent hydrophilic peptides was attempted in presence of EDC. Particle-associated ligands were quantified by fluorescence intensity measurements of the peptide, following purification by dialysis against water. Table 7 zeta potential data of the different particle populations support increased association of peptides in the presence of EDC. However, quantification of associated fluorescence was inconclusive due to significant variability caused by precipitation of PS particles. (Data not shown)

Average Zeta Potential [mV]		
Initial	Control	EDC activated
-60.9 ± 3.31	-59.8 ± 7.56	$0.768 \pm 3.53^*$

Table 7: Characterization of peptide associated PS particles in water.
Data are mean \pm S.D. (n=3) (* $p < 0.0001$)

4.2.4 Transcellular Transplacental Transport

To assess whether surface conjugation of the RGD peptide sequence increases transplacental transport of nanoparticles *in vitro*, we quantified transport of fluorescent PS particles in the absence and presence of surface associated RGD peptide across BeWo cell monolayers cultured on semi-permeable polycarbonate filters (Transwells™). Fluorescence measurements of cumulative apical (AP) → basolateral (BL) flux over 60 minutes were used to calculate permeability coefficient (P_{app}) as described in Materials and Methods. The presence of RGD peptide on PS particles significantly increased particle flux into the receiver compartment, with calculated P_{app} values at $2.14 \pm 0.38 \times 10^{-7}$ cm/s (with RGD peptide) and $6.67 \pm 1.33 \times 10^{-7}$ cm/s (without peptide), respectively. This implies a 3-fold increase in transport properties of peptide-functionalized PS particles.

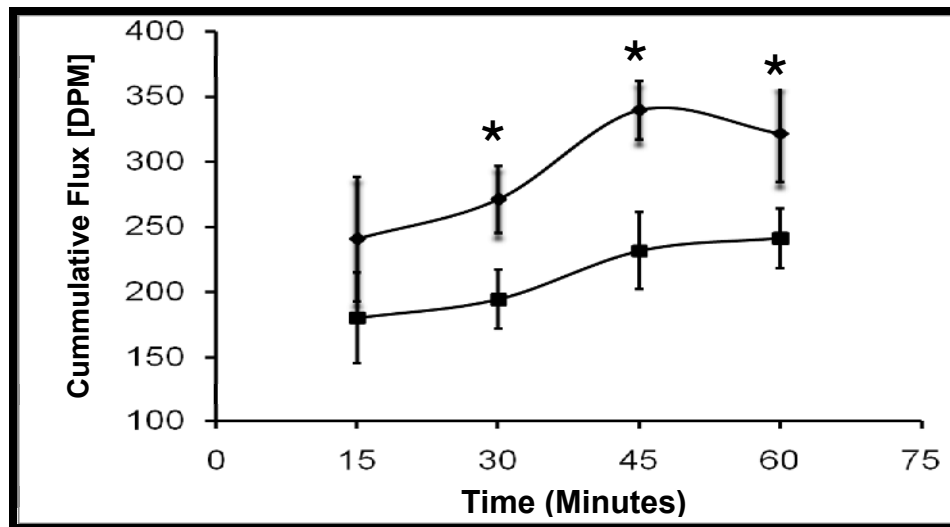


Figure 14: Transport of fluorescent PS particles with and without surface conjugated RGD peptide across BeWo cell monolayers

Cumulative flux over 60 minutes was measured from the AP → BL direction. Data are mean ± S.D. (n=3) (* p < 0.0001)

To support the hypothesis of a receptor mediated transport pathway that becomes accessible by surface-associated RGD peptide, transport studies were performed in presence of 1mM Ac-RY**RGDL**GRR-NH₂ peptide. Inclusion of this metabolically stable peptide effectively reduced the transplacental flux by 20% to a P_{app} value of 5.61 ± 0.36 x 10⁻⁷ cm/s.

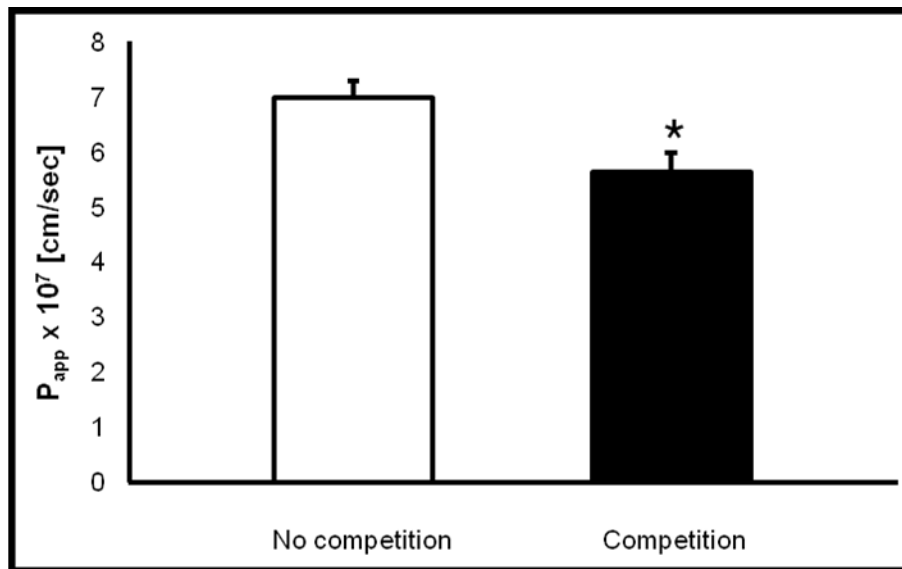


Figure 15: Transport of fluorescent PS particles with surface conjugated RGD peptide across BeWo cell monolayers in absence and presence of 1mM competitive RGD peptide

Cumulative flux over 60 minutes was measured from the AP → BL direction. Data are mean ± S.D. (n=3) (* p < 0.05)

5 Discussion

Targeting of disease sites by polymeric drug delivery systems is dependent on their surface properties. Specific active targeting of these systems can be mediated by ligands expressed on their surfaces. Efficient active targeting by surface expressed peptidic ligands depends not only on their sequences, but also requires optimal numbers to be available in their active forms for interaction with their respective receptors. Through this research, we evaluated design aspects for covalent surface conjugation of ligands to pre-formed polymeric particles.

Aliphatic biocompatible polyesters such as PLGA can be fabricated into nanoparticles with control over surface area, bulk density, surface morphology and sub-cellular particle sizes [28-31]. Commonly reported methods for preparing nanoparticles from biodegradable polymers include solvent evaporation [32], monomer polymerization [33], nano-precipitation [34] and the salting out procedure [35]. We used nano-precipitation, a low energy reproducible method to synthesize uncapped-terminal-end-carboxyl PLGA particles. Diffusion of the PLGA carrying organic phase (acetone) into the aqueous phase causes interfacial turbulence, resulting in rapid particle formation. Precipitation of PLGA in the aqueous medium causes the ionizable carboxyl groups of the polymer to orient themselves towards the surface, while the hydrophobic portions are physically entangled inside the polymerizing nanoparticle matrix [36]. This is demonstrated by the significant negative surface charges of the particles, as represented by the average -45 ± 1.85 mV zeta potential. Consistent average particle diameters at 104 ± 3.5 nm indicate stability of particles under given conditions. Classic colloidal theory states that

electrostatic forces at particle surfaces can cause repulsion and prevent aggregation by virtue of fewer collisions and ionic attractions [36-38].

Addition of buffer salts, required for activation of surface carboxyl groups however caused flocculation of the particles, suggesting a decrease in stability due to reduced electrostatic repulsions. To improve stability under activation conditions, we fabricated the particles in the presence of 0.5% (w/v) polyvinyl alcohol (PVA). PVA, a non-ionic amphiphilic copolymer locates at the interface between particle surface and the aqueous medium during formulation. The hydrophobic segments of PVA penetrate and are entrapped in the polymeric matrix while the hydrophilic segments reduce interfacial tension [39]. Increase in hydrodynamic diameters of the PVA containing particles to 158 ± 2.3 nm in comparison to the no-surfactant particles indicate the presence of PVA chains at particle surfaces. PVA induced steric stabilization is demonstrated by the unchanged average particle diameters under activation conditions. Substantial decrease in the average zeta potential of PVA containing particles to -5.92 ± 0.25 mV is consistent with similar reduction of zeta potential reported for other amphiphilic polymer coated PLGA particles [40]. This decrease in zeta potential can be attributed to shielding of the PLGA surface charges by PVA chains, which is dependent on the PVA concentration used during formulation of the particles. Increasing PVA concentration during formulation can result in greater residual PVA associated with the particles, despite repeated washings [41]. Excess associated PVA can completely cover the surface of the particles making the carboxyl groups inaccessible thereby affecting size, zeta potential, surface hydrophobicity as well as cellular uptake of particles [42].

Controlled conjugation of a known number of ligands to particle surfaces and determination of the reaction efficiency requires accurate quantification of the available carboxyl groups. In past years, acid based and/or conductometric titrations have been used to estimate the amount of carboxyl groups in moles per unit mass of particles [43, 44]. Density of titratable groups per particle could be estimated with knowledge of the polymer density and average particle size. These techniques however, are limited in their application to porous particles, such as fabricated PLGA particles due to their inability to distinguish surface groups from total available groups. To fully explore distribution of the carboxyl groups in porous particles, appropriate sensitive experimental technologies such as isothermal titration calorimetry will be required [45]. However, within the scope of this research, we circumvented this limitation by obtaining non-porous carboxyl functionalized polystyrene particles.

The ease, sensitivity and accuracy of fluorescence labeling for quantitative determination of surface chemical structures of polymers makes it an ideal tool to quantify surface conjugation between particles and ligands [47]. The fluorescent dye, dansyl cadaverine (DC) specifically binds to activated carboxyl groups, through an amide linkage. DC is also characterized by a C₅H₁₀ spacer between the coupling group and the dye, which enables easy access to the primary amine and ensures mobility of the bulky dye. Earlier studies conducted by Farley and colleagues suggest relative insensitivity of DC to its surrounding micro-environment shown by the similarities in the fluorescence emission maxima and quantum yields of surface bound DC and DC in solution [48]. Consequently, using DC as a model ligand, we established surface

conjugation chemistry by direct comparison of fluorescence intensities of particle associated DC, normalized to DC in solution.

For particle surface modification, we evaluated a single step triazine-promoted amidation reaction of carboxylic acids [50, 51]. Adaptation of the technology for surface modification of fabricated PLGA particles however, revealed no significant increase in associated DC in presence of cyanuric chloride. These results are in contrast to successful cyanuric chloride mediated PEG conjugation to PLGA particles, reported by Weiss and colleagues [52]. We hypothesize that PVA chains on fabricated PLGA particle surfaces possibly restrict access of all exposed carboxyl groups to the bulky triazine activation agent. Consequently, changes to particle associated ligands by cyanuric chloride coupling are limited to levels undetectable by DC fluorescence quantification.

EDC, a zero length cross linking agent forms stable intermediates with carboxyl groups in the presence of N-hydroxysuccinimide (NHS) which react with nucleophiles, such as primary amines to form amide bonds. Furthermore, in the absence of primary amines, the activated intermediates hydrolyze back to the free carboxyl form. Aqueous solubility of EDC and NHS limits exposure of PLGA particles to extreme solvent conditions during activation [53]. Increased DC associated on PLGA particles in the presence of EDC after dialysis suggests successful amidation of activated surface carboxyl groups, supported by corresponding decrease in zeta potential. No measured change in zeta potential of PLGA particles in the absence of EDC implies unmodified particle surfaces. However significant associated fluorescence on particles contradicts this inference. We reckon these apparent contradictions to different DC adsorption mechanisms on PLGA

particle surfaces. Non-specific adsorption of DC in the absence of EDC is limited to hydrophobic areas of PLGA particle surfaces, thereby showing no impact on zeta potential. PLGA particle associated DC in presence of EDC is a combination of specific covalent conjugation to carboxyl exposed surface areas, consequently reducing the zeta potential and non-specific adsorption on hydrophobic surface areas.

Hydrophobic non-specific adsorption of DC on PLGA particle surfaces is largely due to its low aqueous solubility. Inefficient separation of non-covalently bound DC by dialysis in water is apparent from molar ratios of associated DC to carboxyl groups. We predicted improved separation of non-specific bound ligands from PLGA particles by increasing solubility in the dialysis vehicle. Use of high concentrations of methanol to increase DC solubility however disrupted PVA induced steric stabilization of particles, illustrated by particle flocculation and aggregation in $\geq 15\%$ (v/v) methanol. Limiting the dialysis vehicle to 10% (v/v) methanol failed to efficiently separate non-covalently bound DC from PLGA on EDC activated particles. Increase in the methanol concentration improved efficiency of separation, as demonstrated by the ultra-filtration study results. Unfortunately, loss of PVA induced steric stabilization and particle smashing due to high gravitational forces caused irreversible aggregation of ultra-filtered particles. Thus, inefficient separation of non-specific bound ligands by appropriate purification techniques without compromising particle stability proved detrimental in use of DC as a model ligand for our research.

We used conductometric titration for quantification of available surface carboxyl groups on PS particles, due to its simplicity and sensitivity to weak and strong acids. Addition of sodium hydroxide to the acid containing sample causes decrease in conductivity, by

virtue of neutralization of the hydrogen ions by hydroxide ions and their replacement by sodium ions. On complete neutralization of all hydrogen ions, further addition of titrant causes increase in conductivity due to the excess sodium ions. Total acid content of sample can be determined by the equivalence point, represented by the intersection of the linearly extrapolated descending and ascending legs of the titration curve. Addition of dilute hydrochloric acid facilitated the accurate determination of the weak equivalence point of the particles by increasing the slopes of the titration curves. The rounded minimum is attributed to the slow attainment of equilibrium near the equivalence point [46]. Estimated carboxyl acid numbers on PS particles were within the range of theoretically expected values calculated from the density and weight information, provided by the supplier (Appendix).

Applicability of the conjugation chemistry to relevant ligands was confirmed by surface modification of particles by a hydrophilic peptide sequence. Relevant peptide analogues were synthesized by solid phase peptide synthesis (SPPS). In SPPS, peptides can be built on small insoluble porous beads through repeated cycles of de-protection and coupling of sequential amino acids. The peptide remains covalently attached to the resin until cleaved by appropriate reagents. By-products from incomplete reactions and/or immature peptide chain termination can also accumulate on the resin, leading to impurities along with the desired peptide. Multiple peaks on HPLC chromatogram(s) of the crude peptide(s) showed presence of impurities. Molecular weight identification of the peptide fragments by spectrometric analysis confirmed the synthesis of target peptide, then purified to > 95 % purity. Elution of the un-acetylated peptide analogue at 5.4 minutes under aqueous conditions implies the hydrophilicity of the peptide

sequence. Competitive peptide analogue, used in transcellular transport assays was synthesized in the acetylated form to prevent degradation by cellular peptidases.

A fluorescent analogue of the truncated peptide sequence was synthesized to evaluate particle surface modification by hydrophilic peptides. Selective de-protection of the ϵ -amine lysine enabled conjugation of FAM to completed peptide sequence, prior to cleavage from resin. Final step coupling of FAM prevented loss of fluorescence properties, by repeated wash cycles during peptide synthesis [49]. Conjugation of FAM on the C-terminal end lysine facilitates easy availability of the dye for fluorescence quantification after N-terminal amidation to particle surface carboxyl groups. Incorporation of FAM causes an increase in the hydrophobicity of the peptide analogue, indicated by a shift of the peak elution to 7.50 minutes on a modified gradient.

The predicted relative ease of separation of non-covalently bound water-soluble ligands from particles led us to choose a hydrophilic peptide sequence as an alternative. No-surfactant PS particles were utilized for evaluation in anticipation of sufficient stability due to their high negative zeta potential determined at -61.7 ± 4.7 mV. Surface modification with a fluorescent analogue of the hydrophilic peptide was attempted on PS particles in presence of EDC. Zeta potential characterization supported increased PS particle peptide association in presence of EDC after dialysis against water. However quantification by fluorescence measurements was inconclusive due to significant variability on account of precipitation of particles. Similar to non PVA containing PLGA particles, flocculation of PS particles could be attributed to reduced surface charges under activation conditions. Moreover, shielding of the stabilizing surface carboxyl

groups by covalently bound peptides and/or possible inter-peptide electrostatic interactions could have also led to particle aggregation.

Active targeting of nanoparticles is dependent on their size and surface properties. Recently, Frenkel and colleagues have demonstrated that particle surface charge can significantly affect internalization mechanisms and intracellular routes [54]. Uptake, distribution and transport of nanoparticles can be through one of several active, energy dependent, saturable endocytosis mechanisms including adsorptive-type endocytosis, transcytosis, and endocytic processes that are neither clathrin- nor caveolin-1 dependent [55-60]. Nanoparticles modified with ligands can show changes in transport properties than their unmodified counterparts due to differences in surface charges and internalization mechanisms. Unmodified particles showed an overall negative charge on account of their free surface carboxylic groups, while the peptide modified particles exhibited a lower zeta potential due to reduced number of surface carboxyl groups. Consistent with this rationale, we demonstrated a 3-fold increase in the transport properties of RGD peptide modified PS particles over unmodified PS particles across an *in vitro* human placenta model. Since positive charges on nanoparticles can stimulate movements towards transcytotic pathways [54], the increased properties of peptide conjugated particles could be partly attributed to reduction in their negative surface charges. The illustrated difference between the transport properties of peptide conjugated and unmodified particles was also shown to be a direct effect of presence of the RGD peptide sequence on particle surfaces. The decrease in flux of RGD peptide conjugated particles in presence of the acetylated peptide analogue in solution clearly suggests receptor mediated pathways of the modified particles. Peptides in solution

compete with the surface bound peptides for the limited saturable receptors resulting in the observed decrease in transport of modified particles. Competition by peptides in solution however only limited the decrease in flux to ~ 80% of the no-competition flux. This limited decrease in flux possibly indicates stronger multivalent interactions between particle bound peptides and receptors counteracting the effect of competing monovalent peptides in solution.

Additionally, due to observed flocculation and aggregation of surface modified particles, we hypothesize that only the smaller nanoparticles are transported across the cells, whereas the bigger aggregated particles precipitate on top of the monolayers. We speculate that control over size and stability would allow comparison of equal diameter particles and would demonstrate a significantly increased difference between the transport properties of the two particle populations. We also anticipate a large difference in transport properties, if a direct comparison were to be made between similarly charged unmodified and peptide modified particles.

In conclusion, through this research we were successful in demonstrating covalent surface modification of particles by peptides without loss of functional activity of the expressed peptides.

6 Future Directions

Surface modification of particles with ligands is intimately linked to their stability. Results from our initial studies with PLGA and PS particles underscore the importance of addressing stabilization of particles when modifying their surface properties. As demonstrated, inherent electrostatic repulsion of particles is often insufficient to maintain original particle sizes under activation conditions. Through careful evaluation of chemical structures and aqueous solubilities of different stabilizers, one could identify an optimal surfactant that could aid in developing a ligand targeted and sterically stabilized nanoparticle formulation for drug delivery. Relevant studies would have to be performed to determine the optimal concentration that would impart stability at the right concentration in buffer conditions without compromising “all” of the functional groups available for conjugation.

Stable polymeric nanoparticles expressing ligands on their surfaces could still suffer from the drawback of shielding of peptides by the polymer, resulting in decrease of peptide density available for receptor binding. Spacers such as PEG chains could then be used between peptides and polymer particles based on the hypothesis that employing extensible PEG chains to tethered peptides may reduce the shielding effect.

The ability of peptide surface modified particles to express characteristics for increased transport across cells *in vitro* was demonstrated in our research. Future studies that focus on confirming this effect explicitly on peptide induced receptor mediated internalization may be required to fully comprehend the impact of valency of surface expressed peptides on optimal targeting and transport of particles across cells.

7 References

1. Panyam, J., *Biodegradable nanoparticles for drug and gene delivery to cells and tissue*. Adv Drug Deliv Rev, 2003. **55**(3): p. 329-47.
2. Florence, A.T., *Transcytosis of nanoparticle and dendrimer delivery systems: evolving vistas*. Adv Drug Deliv Rev, 2001. **50 Suppl 1**: p. S69-89.
3. Choi, S.W., *Design of surface-modified poly(D,L-lactide-co-glycolide) nanoparticles for targeted drug delivery to bone*. J Control Release, 2007. **122**(1): p. 24-30.
4. Brigger, I., *Nanoparticles in cancer therapy and diagnosis*. Adv Drug Deliv Rev, 2002. **54**(5): p. 631-51.
5. Ferrari, M., *Cancer nanotechnology: opportunities and challenges*. Nat Rev Cancer, 2005. **5**(3): p. 161-71.
6. Brissette, R., *Identification of cancer targets and therapeutics using phage display*. Curr Opin Drug Discov Devel, 2006. **9**(3): p. 363-9.
7. Krag, D.N., *Selection of tumor-binding ligands in cancer patients with phage display libraries*. Cancer Res, 2006. **66**(15): p. 7724-33.
8. Shukla, G.S. *Selection of tumor-targeting agents on freshly excised human breast tumors using a phage display library*. Oncol Rep, 2005. **13**(4): p. 757-64.
9. Shukla, G.S., *Phage display selection for cell-specific ligands: development of a screening procedure suitable for small tumor specimens*. J Drug Target, 2005. **13**(1): p. 7-18.
10. Newton, J.R., *In vivo selection of phage for the optical imaging of PC-3 human prostate carcinoma in mice*. Neoplasia, 2006. **8**(9): p. 772-80.
11. Xu, L., *Systemic p53 gene therapy of cancer with immunolipoplexes targeted by anti-transferrin receptor scFv*. Mol Med, 2001. **7**(10): p. 723-34.
12. Bareford, L.M., *Endocytic mechanisms for targeted drug delivery*. Adv Drug Deliv Rev, 2007. **59**(8): p. 748-58.
13. Sergeeva, A., *Display technologies: application for the discovery of drug and gene delivery agents*. Adv Drug Deliv Rev, 2006. **58**(15): p. 1622-54.
14. Ernst J.D., *Phagocytosis of Bacteria and Bacterial Pathogenicity*. Advances in Molecular and Cellular Microbiology, ed. Vol. 12. 2006, New York: Cambridge University Press.

15. Mammen, M., *Polyvalent Interactions in Biological Systems: Implications for Design and Use of Multivalent Ligands and Inhibitors*. Angewandte Chemie International Edition 1998. **37**(20): p. 2754 - 2794.
16. Monsky, W.L., *Augmentation of transvascular transport of macromolecules and nanoparticles in tumors using vascular endothelial growth factor*. Cancer Research 1999. **59**: p. 4129-4135.
17. Winet, H., *Incorporation of polylactide-polyglycolide in a cortical defect: neoangiogenesis and blood supply in a bone chamber*. J Orthop Res, 1995. **13**(5): p. 679-89.
18. Couvreur, P., *Nanotechnology: intelligent design to treat complex disease*. Pharm Res, 2006. **23**(7): p. 1417-50.
19. Moghimi, S.M., *Nanomedicine: current status and future prospects*. FASEB J, 2005. **19**(3): p. 311-30.
20. Hartig, S.M., *Multifunctional nanoparticulate polyelectrolyte complexes*. Pharm Res, 2007. **24**(12): p. 2353-69.
21. Costantino, L., *Peptide-derivatized biodegradable nanoparticles able to cross the blood-brain barrier*. J Control Release, 2005. **108**(1): p. 84-96.
22. Kocbek, P., *Targeting cancer cells using PLGA nanoparticles surface modified with monoclonal antibody*. J Control Release, 2007. **120**(1-2): p. 18-26.
23. Sahoo, S.K., *Enhanced antiproliferative activity of transferrin-conjugated paclitaxel-loaded nanoparticles is mediated via sustained intracellular drug retention*. Mol Pharm, 2005. **2**(5): p. 373-83.
24. Mo, Y., *Mechanistic study of the uptake of wheat germ agglutinin-conjugated PLGA nanoparticles by A549 cells*. J Pharm Sci, 2004. **93**(1): p. 20-8.
25. Astete, C.E., *Synthesis and characterization of PLGA nanoparticles*. J Biomater Sci Polym Ed, 2006. **17**(3): p. 247-89.
26. Shaik, S.B., *Integrin-binding peptide facilitate transcytosis of T7 bacteriophages across the human placenta in vitro*. AAPS National Biotechnology Conference, June 24-27, San Diego, CA, 2007.
27. Bodmeier, R., *Solvent selection in the preparation of poly(DL-lactide) microspheres prepared by the solvent evaporation method*. International Journal of Pharmaceutics, 1988. **43**: p. 179-186.

28. Saunders, R.A., *Coated Vicryl (polyglactin 910) suture in extraocular muscle surgery*. *Ophthalmic Surg*, 1979. **10**(7): p. 13-8.
29. Guerin, C., *Recent advances in brain tumor therapy: local intracerebral drug delivery by polymers*. *Invest New Drugs*, 2004. **22**(1): p. 27-37.
30. Avgoustakis, K., *PLGA-mPEG nanoparticles of cisplatin: in vitro nanoparticle degradation, in vitro drug release and in vivo drug residence in blood properties*. *J Control Release*, 2002. **79**(1-3): p. 123-35.
31. Caron, P., *Somatuline(R) Autogel(R), a new formulation of lanreotide for the treatment of acromegalic patients*. *Annales d'endocrinologie* 2002. **63**: p. 2S19-2S24.
32. Song, C., *Dexamethasone-nanoparticles for intra-arterial localization in restenosis in rats*. *Proceedings of the International Symposium on Controlled Release* 1995. **22**: p. 444-445.
33. Harmia, T., *A solid colloidal drug delivery system for the eye: encapsulation of pilocarpin in nanoparticles*. *J Microencapsul*, 1986. **3**(1): p. 3-12.
34. Molpeceres, J., *Application of central composite designs to the preparation of polycaprolactone nanoparticles by solvent displacement*. *J Pharm Sci*, 1996. **85**(2): p. 206-13.
35. Allemann, E., *In vitro extended-release properties of drug-loaded poly(DL-lactic acid) nanoparticles produced by a salting-out procedure*. *Pharm Res*, 1993. **10**(12): p. 1732-7.
36. Govender, T., *PLGA nanoparticles prepared by nanoprecipitation: drug loading and release studies of a water soluble drug*. *Journal of Controlled Release* 1999. **57**: p. 171-185.
37. Sugrue, S., *Predicting and controlling colloid suspension stability using electrophoretic mobility and particle size measurements*: *American laboratory* 1992. **24**(6): p. 64-71.
38. Trimaille, T., *Poly(D,L-lactic acid) nanoparticle preparation and colloidal characterization*. *Colloid Polymer Science*, 2003. **281**(12): p. 1184-1190.
39. Boury, F., *Dynamic properties of poly (DL-lactide) and polyvinyl alcohol monolayers at the air/water and dichloromethane/water interfaces* 1995. **169**: p. 380-392.

40. Redhead, H.M., *Drug delivery in poly(lactide-co-glycolide) nanoparticles surface modified with poloxamer 407 and poloxamine 908: in vitro characterisation and in vivo evaluation*. J Control Release, 2001. **70**(3): p. 353-63.
41. Sahoo, S.K., *Residual polyvinyl alcohol associated with poly (D,L-lactide-co-glycolide) nanoparticles affects their physical properties and cellular uptake*. J Control Release, 2002. **82**(1): p. 105-14.
42. Feczko, T., *Comparison of the preparation of PLGA-BSA nano- and microparticles by PVA, poloxamer and PVP*. Physicochemical and Engineering Aspects 2008. **319**(1-3): p. 188-195.
43. Hoare, T., *Functional group distributions in carboxylic acid containing poly(N-isopropylacrylamide) microgels*. Langmuir, 2004. **20**(6): p. 2123-33.
44. Kang, K., *Control of particle size and carboxyl group distribution in soap-free emulsion copolymerization of methyl methacrylate-ethyl acrylate-acrylic acid* Journal of Applied Polymer Science. **92**(1): p. 433-438.
45. Okubo, M., *Estimation of distribution state of carboxyl groups within submicron-sized, carboxylated polymer particle with isothermal titration calorimeter*. Colloid & Polymer Science, 2006. **284**(11).
46. Hul, V.D., *The characterization of latex particle surfaces by ion exchange and conductometric titration*. Journal of Electroanalytical Chemistry, 1972. **37**: p. 161.
47. Ivanov, V.B., *Determination of Functional Groups on Polymer Surfaces Using Fluorescence Labeling*. Surface and Interface Analysis, 1996. **24**: p. 251-262.
48. Holmes-Farley, S.R., *Fluorescence Properties of Dansyl Groups Covalently Bonded to the Surface of Oxidatively Functionalized Low-Density Polyethylene Film* Langmuir, 1986(2): p. 266-281.
49. Fernandez-Carneado, J., *An efficient method for the solid-phase synthesis of fluorescently labeled peptides*. Tetrahedron Letters 2004. **45**: p. 6079-6081.
50. Moghimi, S.M., *Chemical camouflage of nanospheres with a poorly reactive surface: towards development of stealth and target-specific nanocarriers*. Biochim Biophys Acta, 2002. **1590**(1-3): p. 131-9.
51. Rayle, H.L., *Development of a Process for Triazine-Promoted Amidation of Carboxylic Acids*. Organic Process Research & Development, 1999 **3**: p. 172-176.

52. Weiss, B., *Coupling of biotin-(poly(ethylene glycol))amine to poly(D,L-lactide-co-glycolide) nanoparticles for versatile surface modification*. *Bioconjug Chem*, 2007. **18**(4): p. 1087-94.
53. Staros, J.V., *Enhancement by N-hydroxysulfosuccinimide of water-soluble carbodiimide-mediated coupling reactions*. *Anal Biochem*, 1986. **156**(1): p. 220-2.
54. Frenkel, O.H., *Surface Charge of Nanoparticles Determines Their Endocytic and Transcytotic Pathway in Polarized MDCK Cells*. *Biomacromolecules*, 2008. **9**: p. 435–443.
55. Fiegel, J., *Large porous particle impingement on lung epithelial cell monolayers--toward improved particle characterization in the lung*. *J. Pharm Res*. 2003. **20**: p.788–796.
56. Behrens, I., *Comparative uptake studies of bio-adhesive and non-bio-adhesive nanoparticles in human intestinal cell lines and rats: The effect of mucus on particle adsorption and transport*. *Pharm. Res*. 2002. **19**: p.1185–1193.
57. Panyam, J., *Dynamics of endocytosis and exocytosis of poly(D,L-lactide-co-glycolide) nanoparticles in vascular smooth muscle cells*. *Pharm. Res*. 2003. **20**: p. 212–220.
58. Panyam, J., *Rapid endo-lysosomal escape of poly(dl-lactide-co-glycolide) nanoparticles: implications for drug and gene delivery*. *FASEB J*. 2002. **16**: p. 1217–1226
59. Frenkel, O.H., *Targeting of nanoparticles to the clathrin-mediated endocytic pathway*. *Biochem. Biophys. Res. Commun*. 2007. **353**. p.26–32.
60. Mao, S., *Uptake and transport of PEG-graft-trimethyl-chitosan copolymer-insulin nanocomplexes by epithelial cells*. *Pharm. Res*. 2005. **22**: p.2058–2068.
61. Novotna, M., *P-glycoprotein in the placenta: Expression, localization, regulation and function*. *Reprod. Toxicol*. 2006. **22**: p.400-410
62. Young, A., *Efflux transporters of the human placenta*. *Adv Drug Deliv Rev.*, 2003. **55**: p.125-132
63. Hay, W., *Placental transport of nutrients to the fetus*. *Horm. Res*. 1994. **42**: p.215–222.
64. Van der Ende, A., *Modulation of transferrin-receptor activity and recycling after induced differentiation of BeWo choriocarcinoma cells*. *Biochem. J*. 1990. **270**: p.451–457.

8 Appendix

Theoretical calculation of available carboxyl groups on Polystyrene particles

Manufacturer's Specifications:

Diameter: [1.26 μ (Range: 1.0 μ - 1.4 μ)]

Concentration: 5% (w/v)

Surface coverage: One carboxyl group per 25 \AA^2

Nomenclature:

W = Weight of polymer in (gm)

P = Density of polymer (Polystyrene = 1.05)

D = Diameter of particles (μm)

N = Number of particles

A = Surface area of particles (cm^2)

Avogadro's Number: 6.02×10^{23}

Equations:

$$N = \left[\frac{6 \times W}{(3.14 \times P \times D^3)} \right] \times 10^{12}$$

$$A = \left[\frac{(6 \times W)}{(P \times D)} \right] \times 10^4$$

	Minimum	Maximum	Average
Number of particles	16.58×10^9	45.49×10^9	22.74×10^9
Surface area of particles (\AA^2)	1020.41×10^{16}	1428.57×10^{16}	1133.78×10^{16}
Total carboxyl groups (μmoles)	0.678	0.949	0.7533
